






Harmonization of Quantitative Parenchymal Enhancement in T₁-Weighted Breast MRI

Bas H.M. van der Velden, PhD,^{1*}  Michael J. van Rijssel, PhD,¹  Beatrice Lena, MSc,¹
 Marielle E.P. Philippens, PhD,²  Claudette E. Loo, MD, PhD,³ Max A.A. Ragusi, MD,¹ 
 Sjoerd G. Elias, MD, PhD,⁴ Elizabeth J. Sutton, MD,⁵ Elizabeth A. Morris, MD,⁵ 
 Lambertus W. Bartels, PhD,¹ and Kenneth G.A. Gilhuijs, PhD¹

Background: Differences in imaging parameters influence computer-extracted parenchymal enhancement measures from breast MRI.

Purpose: To investigate the effect of differences in dynamic contrast-enhanced MRI acquisition parameter settings on quantitative parenchymal enhancement of the breast, and to evaluate harmonization of contrast-enhancement values with respect to flip angle and repetition time.

Study Type: Retrospective.

Phantom/Populations: We modeled parenchymal enhancement using simulations, a phantom, and two cohorts ($N = 398$ and $N = 302$) from independent cancer centers.

Sequence Field/Strength: 1.5T dynamic contrast-enhanced T₁-weighted spoiled gradient echo MRI. Vendors: Philips, Siemens, General Electric Medical Systems.

Assessment: We assessed harmonization of parenchymal enhancement in simulations and phantom by varying the MR parameters that influence the amount of T₁-weighting: flip angle (8°–25°) and repetition time (4–12 msec). We calculated the median and interquartile range (IQR) of the enhancement values before and after harmonization. In vivo, we assessed overlap of quantitative parenchymal enhancement in the cohorts before and after harmonization using kernel density estimations. Cohort 1 was scanned with flip angle 20° and repetition time 8 msec; cohort 2 with flip angle 10° and repetition time 6 msec.

Statistical Tests: Paired Wilcoxon signed-rank-test of bootstrapped kernel density estimations.

Results: Before harmonization, simulated enhancement values had a median (IQR) of 0.46 (0.34–0.49). After harmonization, the IQR was reduced: median (IQR): 0.44 (0.44–0.45). In the phantom, the IQR also decreased, median (IQR): 0.96 (0.59–1.22) before harmonization, 0.96 (0.91–1.02) after harmonization. Harmonization yielded significantly ($P < 0.001$) better overlap in parenchymal enhancement between the cohorts: median (IQR) was 0.46 (0.37–0.58) for cohort 1 vs. 0.37 (0.30–0.44) before harmonization (57% overlap); and 0.35 (0.28–0.43) vs. 0.37 (0.30–0.44) after harmonization (85% overlap).

Data Conclusion: The proposed practical harmonization method enables an accurate comparison between patients scanned with differences in imaging parameters.

Level of Evidence: 3

Technical Efficacy Stage: 4

J. MAGN. RESON. IMAGING 2020;52:1374–1382.

DYNAMIC CONTRAST-ENHANCED magnetic resonance imaging (MRI) is the principal sequence in breast MRI for assessment of breast cancer.¹ Healthy breast parenchymal tissue

also demonstrates contrast-enhancement on MRI. This background parenchymal enhancement (BPE) is increasingly used in the context of cancer diagnosis, prognosis, and risk assessment.^{2,3}

View this article online at wileyonlinelibrary.com. DOI: 10.1002/jmri.27244

Received Mar 9, 2020, Accepted for publication May 20, 2020.

*Address reprint requests to: B.H.M.v.d.V., Q.02.4.45, P.O. Box 85500, 3508 GA Utrecht, The Netherlands. E-mail: bvelden2@umcutrecht.nl

Contract grant sponsor: the Dutch Cancer Society (KWF); Contract grant number: 10755.

Level of Evidence Technical Efficacy Stage

From the ¹Image Sciences Institute, University Medical Center Utrecht, Utrecht University, Utrecht, The Netherlands; ²Department of Radiotherapy, University Medical Center Utrecht, Utrecht University, Utrecht, The Netherlands; ³Department of Radiology, The Netherlands Cancer Institute – Antoni van Leeuwenhoek Hospital, Amsterdam, The Netherlands; ⁴Julius Center for Health Sciences and Primary Care, University Medical Center Utrecht, Utrecht University, Utrecht, The Netherlands; and ⁵Department of Radiology, Memorial Sloan Kettering Cancer Center, New York, New York, USA

This is an open access article under the terms of the Creative Commons Attribution-NonCommercial-NoDerivs License, which permits use and distribution in any medium, provided the original work is properly cited, the use is non-commercial and no modifications or adaptations are made.

Assessment of breast MRI follows guidelines from the Breast Imaging Reporting and Data System (BI-RADS).⁴⁻⁷ These guidelines address standardization of image acquisition parameters such as the timing of the postcontrast images.⁴ They do not, however, address imaging parameter settings such as the values of the flip angle and repetition time (TR).⁴ These parameters influence the signal intensity in spoiled gradient echo imaging, the most commonly used imaging technique in breast dynamic contrast-enhanced MRI.¹ Therefore, differences in parameters will influence computer-extracted measures from these images.⁸

Recently, several researchers suggested computer-extracted measures to quantify BPE.⁹⁻¹⁷ These measurements are inherently sensitive to differences in imaging parameter settings, complicating pooling of results across studies. For example, two studies reporting an association between parenchymal enhancement of the contralateral breast and patient survival used cohort-specific data-driven cutoffs.^{18,19} In a recent prospective multicenter study, computer-extracted biomarkers based on contrast enhancement needed to be manually adjusted to account for variability in the MRI system and scan protocol.⁸ Since it is difficult to prospectively account for all variation in multicenter studies, post-hoc harmonization of enhancement biomarkers is of interest (ie, the process of achieving a consistent value regardless of imaging protocol).

Taking the above into account, we aimed to investigate the effect of differences in MRI acquisition parameter settings on quantitative parenchymal enhancement. Furthermore, we evaluated a harmonization method to adjust the differences in enhancement caused by differences in parameters.

Material and Methods

Simulation

Contralateral parenchymal enhancement (CPE) is defined as the top 10% relative signal-enhancement between the first and the last postcontrast scan in dynamic contrast-enhanced MRI (Fig. 1).¹⁸ We simulated the image intensities of breast parenchymal tissue at three timepoints in a contrast-enhanced series: precontrast, first postcontrast (eg, 90 seconds after contrast injection), and last postcontrast (eg, 360 seconds after contrast injection) (Fig. 1).

We simulated the parenchymal tissue at known quantitative T_1 values at 1.5T.²⁰ We modeled the signal of the precontrast parenchyma using 1000 voxel values with a T_1 value of 1246 msec. We used a range of T_1 values in the postcontrast simulations since the parenchyma typically shows heterogeneity of signal enhancement in response to contrast influx.²¹

We chose a T_1 ranging from 959–1149 msec for the first postcontrast series, and 597–892 msec for the last postcontrast series. The ranges decrease over time because the

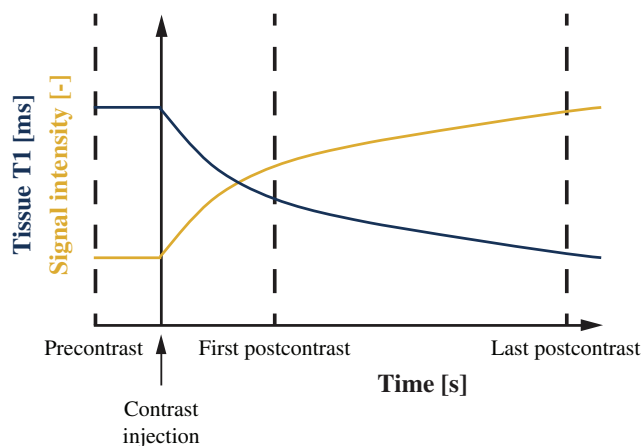


FIGURE 1: Illustration of the continuous decrease of T_1 in the breast parenchyma (vertical axis, blue line) over time (horizontal axis) after contrast injection. As a result of decreasing T_1 , the signal intensity in these voxels increases (vertical axis, gold line). The parenchymal enhancement biomarker is defined as the top-10% relative increase between the first and last postcontrast scan.

concentration of gadolinium after contrast typically continues to increase in parenchymal tissue (Fig. 1).

We simulated the signal using the steady-state spoiled gradient echo signal equation,²² and added Gaussian noise to the signal with a signal-to-noise ratio (SNR) comparable to our phantom measurements (ie, 25, 28, and 45 for pre-, first post-, and last postcontrast, respectively). We simulated this signal using a range of imaging parameter settings resembling those used in clinical protocols: TRs between 4 and 12 msec and flip angles between 8° and 25° .^{18,23-25} Proton density and TE were kept constant.

We assessed the effect of SNR on the ability to accurately correct parenchymal enhancement. For this, we simulated the precontrast and postcontrast signals with increasing noise levels, and recorded at which noise level the error between the harmonized CPE and the reference CPE (ie, flip angle 10° , TR 4 msec) became higher than 10%.

Furthermore, we assessed the effect of B_1^+ field inhomogeneities using a similar method, by recording at what field inhomogeneity the error between the harmonized CPE and the reference CPE (ie, flip angle 10° , TR 4 msec) became higher than 10%. We simulated the inhomogeneities using both a bias and deviations from the nominal flip angle. The bias of the simulated B_1^+ field inhomogeneities was set at 120%,²⁶ while ranging the absolute deviations from this bias between 0% and 100%. Hence, a B_1^+ inhomogeneity of 40% refers to a B_1^+ field ranging between 80% and 160%, with the average at 120%.

Phantom

We measured parenchymal enhancement using a calibrated phantom containing a series of materials with known relaxation times (Test object 5, Eurospin II Test System, Diagnostic Sonar, Edinburgh, UK).

The phantom included a set of 18 calibrated test tubes. Each tube is filled with doped polysaccharide gel and provides specific relaxation times at specified temperatures and magnetic field strengths. We defined three signals using these tubes: one signal consisted of a “precontrast tube” mimicking parenchymal tissue without contrast, and two consisted of “postcontrast tubes” mimicking the gradual decrease of T_1 (Fig. 1). We chose the tube calibrated at a T_1 of 1246 msec as the precontrast tube. We chose the tubes calibrated at a T_1 of 1149, 1023, and 959 msec as the first postcontrast tubes, and the tubes at a T_1 of 892, 745, and 597 as the last postcontrast tubes.

We approximated dynamic contrast-enhanced MRI in the phantom using different tubes at known T_1 values. Hence, our timepoints (ie, precontrast, first postcontrast, and last postcontrast) were actually different locations in the MR image. These spatial variations may influence the measurements because of differences in the B_1^+ field and may therefore influence the adjustment of parenchymal enhancement. We showed the effect of these spatial variations by using the actual flip angle in our harmonization, which was the flip angle multiplied by the scaling of the B_1^+ field at that location.

MRI

We imaged the phantom using a 1.5T MR unit (Achieva, Philips, Best, The Netherlands). We used a dedicated breast MR coil (SENSE 7 Breast coil, Philips) and performed spoiled gradient echo imaging using the same range of clinically used imaging parameter as in the simulation.^{18,23–25} Other imaging parameters were: echo time (TE) 1.7 msec, voxel size $1 \times 1 \times 1 \text{ mm}^3$, and image dimension $224 \times 224 \times 50$ voxels. We assessed the SNR of the MR image by measuring the noise of the phantom using a scan without gradients and radiofrequency pulses at TR of 4 msec and flip angle of 10° .²⁷ We acquired a B_1^+ -map to assess the actual flip angle (actual flip angle imaging, TRs 30 and 150 msec, TE 2.4 msec, flip angle 60° , resolution $2 \times 2 \times 4 \text{ mm}^3$).²⁸

Image Analysis

We automatically extracted the calibrated tubes from the MR image using a threshold based on Otsu’s method²⁹ and labeled them with a connected component analysis, yielding a binary mask per tube. We eroded the binary masks (radius of two voxels) to account for partial volume effects along the borders.

To assess parenchymal enhancement, we used the previously defined signal-tubes: the precontrast tube, the first postcontrast tubes, and the last postcontrast tubes. From the latter tubes, we randomly sampled the same number of voxels (ie, 5201 voxels) yielding a total of 15,603 voxel values from which we calculated the CPE.

Harmonization of Parenchymal Enhancement

We harmonized parenchymal enhancement for differences in TR and flip angle based on the method proposed by Haacke et al.²² First, we assessed the T_1 value of each voxel in the parenchyma at the postcontrast image²²:

$$T_1(t) = \frac{-TR}{\ln\left(\frac{x-y}{x-y\cos\alpha}\right)}$$

with:

$$y = \frac{S(t)}{S(0)}$$

$$x = \frac{1 - e^{-\frac{TR}{T_1(0)}} \cos\alpha}{1 - e^{-\frac{TR}{T_1(t)}}}$$

where $S(0)$ is the signal of the precontrast image, $S(t)$ the signal at the postcontrast image at timepoint t , $T_1(0)$ the T_1 value in without contrast agent, TR the repetition time, and α the flip angle.

After obtaining $T_1(t)$, we calculated the simulated signal \hat{S} in each voxel of the parenchymal tissue as if they were imaged with different repetition time (TR_{new}) and flip angle (α_{new}):

$$\hat{S}(t, \alpha_{new}, TR_{new}) = \frac{\sin\alpha_{new} \left(1 - e^{-\frac{TR_{new}}{T_1(t)}}\right)}{1 - \cos\alpha_{new} \cdot e^{-\frac{TR_{new}}{T_1(t)}}}$$

We chose a TR of 4 msec and flip angle 10° .

We performed these steps for both the first postcontrast and the last postcontrast signal. From these new adjusted postcontrast signals, the adjusted parenchymal enhancement was calculated using the same CPE definition.

All harmonization steps were performed in Python 3.7.4.

Clinical Data

We evaluated CPE using two previously reported cohorts with a total of 696 patients.^{18,19} Institutional Review Board (IRB) approvals were obtained for the analyses of patient data^{18,19}; written informed consent was obtained¹⁸ or waived by the IRB.¹⁹ Both cohorts solely included patients with unilateral estrogen receptor-positive/HER2-negative breast cancer who received a preoperative dynamic contrast-enhanced T_1 -weighted MRI of both breasts. All patients were eligible for breast-conserving surgery based on conventional imaging and clinical examination (Table 1). CPE was calculated in parenchymal tissue voxels on dynamic contrast-enhanced MRI, which were automatically segmented in 3D (Fig. 2, see^{18,19} for implementation details) (Table 1).

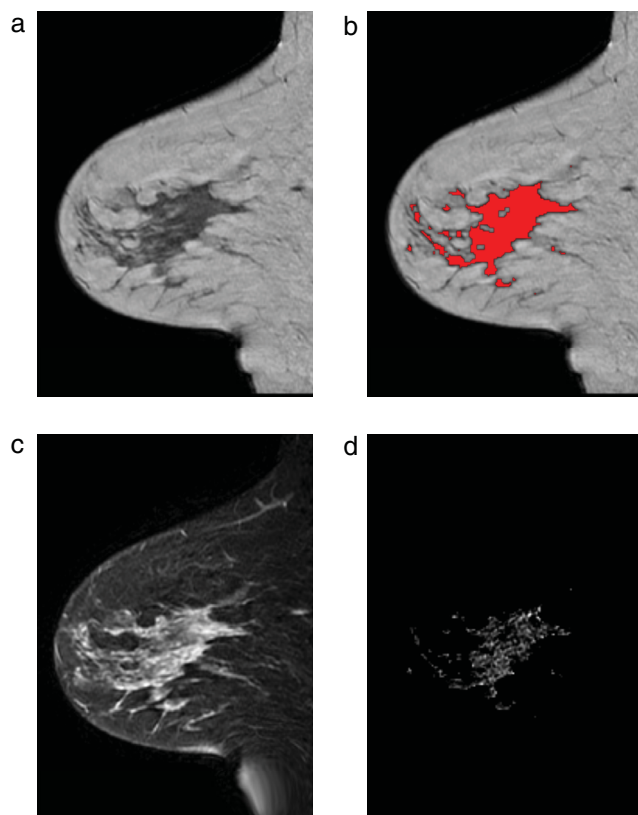


FIGURE 2: Example of the image processing from cohort 2 in the contralateral breast of a 42-year-old patient with an ER-positive/HER2-negative invasive ductal carcinoma in the right breast. (a) Sagittal T₁-weighted image. (b) Same image with parenchymal tissue overlaid in red. (c) Fat-suppressed first postcontrast image. (d) Enhancement in the parenchymal tissue segmentation.

Notable differences in MRI acquisition between these two patient cohorts were the discrepancies in vendor, flip angle, and TR. Cohort 1 was scanned on a Siemens MR unit with TR of 8.0 msec and flip angle of 20°, whereas cohort 2 was scanned on a General Electric Medical Systems (Milwaukee, WI) MR unit with TR of 6.0 msec and flip angle 10° (Table 2).

To assess whether our clinical data have the required SNR for harmonization, we calculated the SNR in the parenchymal tissue using manual annotations in 10 patients (Table 3). The signal was assessed in the parenchymal tissue of the first postcontrast image; the noise was assessed as a Rician distribution in the air.³⁰

Statistical Analysis

We assessed the effect of harmonization on the simulations and phantom using the median and interquartile range (IQR). We tested the similarity of the CPE distributions in the two cohorts using the overlap of the kernel density estimations,³¹ and tested the improvement of overlap after harmonization using the paired Wilcoxon signed rank test after bootstrapping. We considered the results statistically significant when the two-sided *P*-value was under 0.05.

TABLE 1. Patient Characteristics

Characteristic	Cohort 1 (<i>N</i> = 398)	Cohort 2 (<i>N</i> = 302)
Age at diagnosis (years) ^a	58 (50–64)	48 (42–57)
Largest tumor diameter (cm) ^a	1.7 (1.2–2.5)	1.3 (0.8–1.9)
Histological grade (%)		
Grade I	161 (41)	26 (9)
Grade II	181 (46)	106 (35)
Grade III	44 (11)	157 (52)
Unknown	8 (2)	13 (4)
Progesterone receptor		
Negative	99 (25)	49 (16)
Positive	294 (75)	253 (84)
Unknown	1 (0)	0 (0)
Axillary load (%)		
0 positive lymph nodes	265 (67)	166 (55)
1–3 positive lymph nodes	101 (26)	99 (33)
4 or more positive lymph nodes	24 (6)	36 (12)
Unknown	4 (1)	1 (0)
All patients had unilateral estrogen receptor-positive/HER2-negative breast cancer. Values represent number of patients (percentages).		
^a Values represent median value (interquartile range).		

Statistical analyses were performed using R 3.6.1. (R Foundation for Statistical Computing, Vienna, Austria).

Results

Simulation

As shown in Fig. 3, the simulated parenchymal enhancement increased with increasing flip angle and decreased with increasing TR. Before harmonization, simulated parenchymal enhancement values had a median (IQR) value of 0.46 (0.34–0.49). After harmonization, the IQR reduced: median (IQR): 0.44 (0.44–0.45) (Fig. 3).

The error to the reference parenchymal enhancement value (flip angle 10°, TR 4 msec) after harmonization was lower than 10% in most clinically used parameter settings for commonly used SNRs (Fig. 4) and for clinically expected B₁⁺ field inhomogeneities (Fig. 5).

TABLE 2. MRI Characteristics

Characteristic	Cohort 1 (N = 398)	Cohort 2 (N = 302)
Field strength (T)	1.5	1.5
Vendor	Siemens	General Electric Medical Systems
Sequence	Spoiled gradient echo	Spoiled gradient echo
Repetition time (msec)	8.0	6.0
Echo time (msec)	4.0	4.2
Flip angle (°)	20	10
Contrast agent	Prohance (Bracco-Byk Gulden)	Magnevist (Bayer Health Care Pharmaceuticals)
Injected dose (mmol/kg)	0.1	0.1
Duration of dynamic contrast-enhanced series (s)	360	360
Voxel size (mm ³)	1.35 × 1.35 × 1.35	0.7 × 0.7 × 3.0
Matrix size	256 × 256 × 100	256 × 256 × 100
Fat suppression	No	Yes

TABLE 3. Signal-to-Noise Ratios in 10 Patients From Cohort 1

Patient Study ID	SNR
1	15.4
2	11.2
3	13.5
4	15.1
5	13.8
6	18.3
7	21.4
8	15.0
9	17.1
10	17.7
Mean (SD)	15.9 (2.7)

Phantom

We observed similar behavior in the phantom as in the simulation: signal enhancement values increased with increasing flip angle and decreased with increasing TR (Fig. 6).

Before harmonization, signal enhancement values measured in the phantom had a median (IQR) of 0.96 (0.59–1.22). After harmonization, the IQR decreased: median (IQR): 0.91 (0.86–0.98) without mitigating B_1^+ inhomogeneities,

median (IQR): 0.96 (0.91–1.02) with mitigating B_1^+ inhomogeneities.

The SNR was 25 in the precontrast tube, 28 in the first postcontrast tubes, and 46 in the last postcontrast tubes. The median actual flip angle was above 90° and below 110° in all tubes.

Clinical Data

Consistent with the simulation and phantom, CPE was higher at a flip angle of 20° and TR of 8 msec (cohort 1, median [IQR]: 0.46 [0.37–0.58]) compared to using flip angle of 10° and TR of 6 msec (cohort 2, median [IQR]: 0.37 [0.30–0.44], Fig. 7). After harmonization of cohort 1 to the parameter settings of cohort 2, the distribution in cohort 1 better resembled cohort 2 (median [IQR]: 0.35 [0.28–0.43], Fig. 7). The overlap of the kernel density estimations significantly increased from 57% (95% confidence interval [CI]: 49–63%) to 85% (95% CI: 73–89%) after harmonization ($P < 0.001$). The mean SNR that we measured in the parenchymal tissue of patients was 15.9 with a standard deviation (SD) of 2.7 (Table 3).

Discussion

We demonstrated that harmonization of parenchymal enhancement values is needed to ensure an accurate comparison between patients scanned with different dynamic contrast-enhanced MRI acquisition parameter settings. We proposed a harmonization method to adjust differences in parenchymal enhancement caused by differences in these parameters. Additionally, we showed that the CPE observed

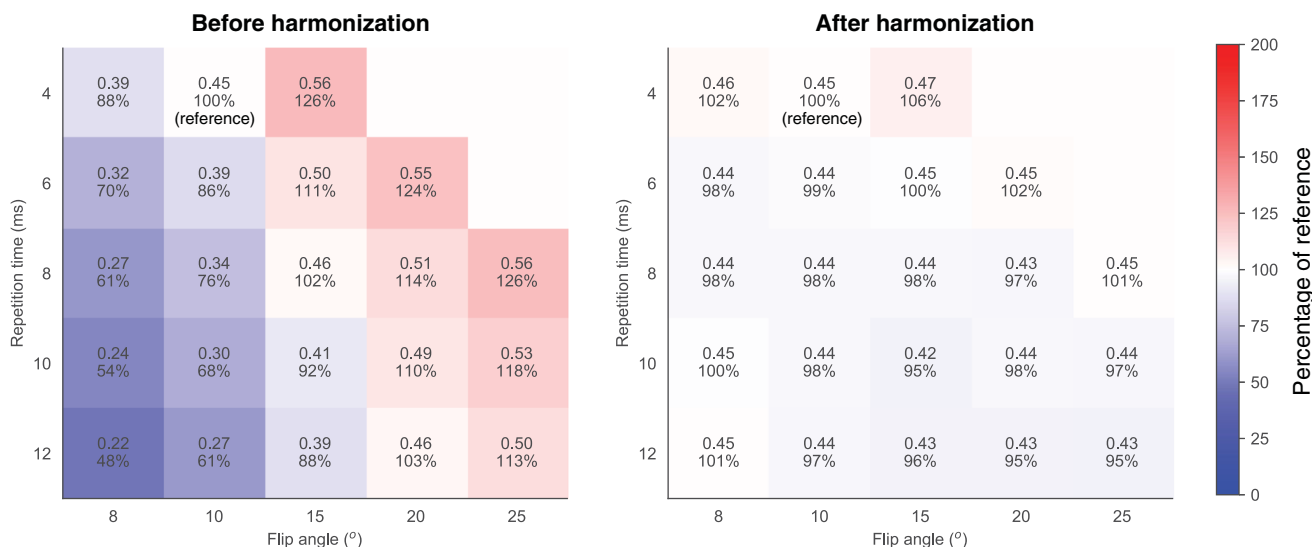


FIGURE 3: Parenchymal enhancement simulated at various flip angles and TRs before (left) and after harmonization (right). The reference situation was at flip angle of 10° and TR of 4 msec. The median (interquartile range (IQR)) of the simulations was 0.46 (0.34–0.54) before harmonization (left image) and 0.44 (0.44–0.46) after harmonization (right image). The colors are based on the percentages compared to the reference.

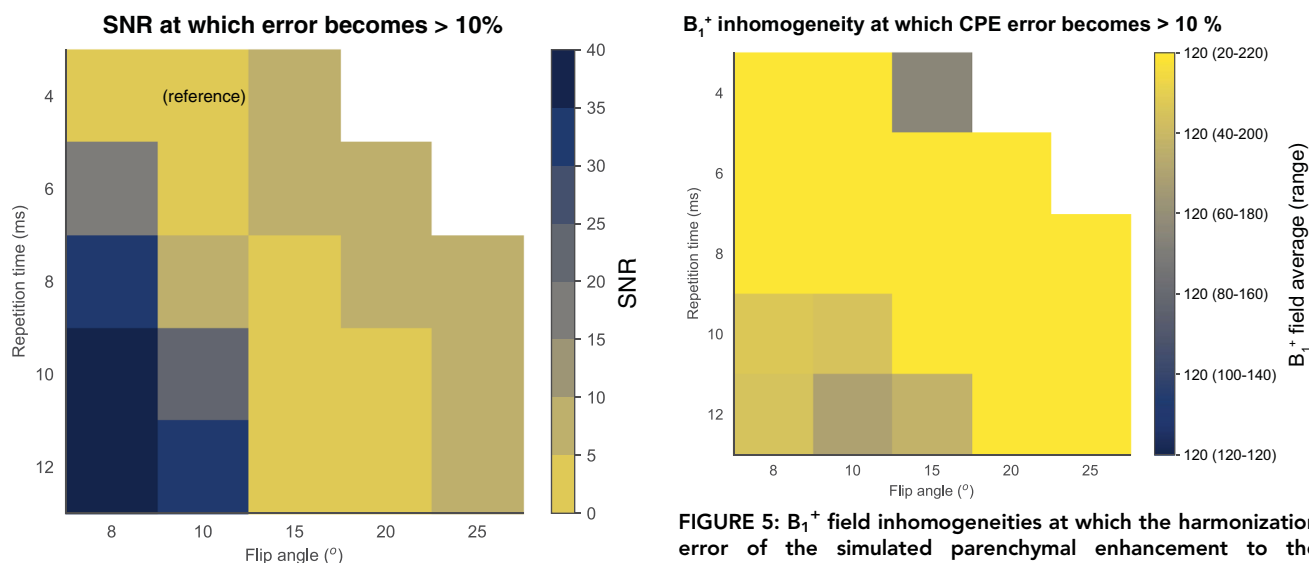


FIGURE 4: Minimum required SNRs to be able to harmonize simulated parenchymal enhancement to the reference (flip angle 10°, TR 4 msec). Acceptable limits were chosen at 10% error from the reference. It is feasible to adjust parenchymal enhancement to the reference if the SNR is higher than 5 to 10 (yellow diagonal band).

in two patient cohorts was equivalent after harmonization. These results suggest that pooling of data in multi-institutional studies is feasible after correction of enhancement values.

Differences in image acquisition parameter settings influence computer-extracted measures of dynamic contrast-enhanced MRI.⁸ In addition to complicating pooling of data across studies, it also complicates correctly classifying prospectively acquired subject data, hindering research into personalized healthcare. Therefore, it is desirable to produce the same

value for such biomarkers regardless of acquisition parameters. One way to achieve such harmonization is by strict guidelines or community-wide harmonization efforts.^{4,5} While these guidelines are important for established biomarkers, they are unfeasible for relatively novel biomarkers. Only more established biomarkers are likely to receive the required support from the scientific and clinical community to a priori harmonize relevant parameters between centers. Therefore, post-hoc harmonization of relatively novel biomarkers is of interest.

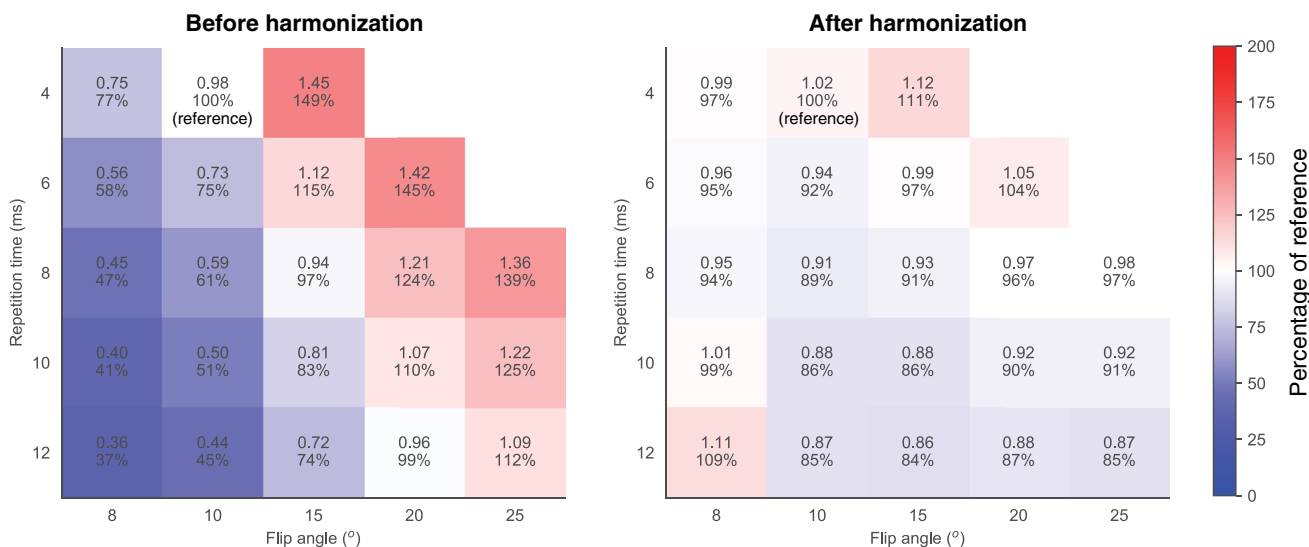


FIGURE 6: Parenchymal enhancement measured in the phantom at various flip angles and TRs before (left) and after harmonization (right). The reference situation was at flip angle of 10° and TR of 4 msec. The median (IQR) of the measurements was 0.96 (0.59–1.22) before harmonization (left figure) and 0.96 (0.91–1.02) after harmonization and mitigation of B₁⁺ inhomogeneities (right figure). The colors are based on the percentages compared to the reference comparable to Fig. 3.

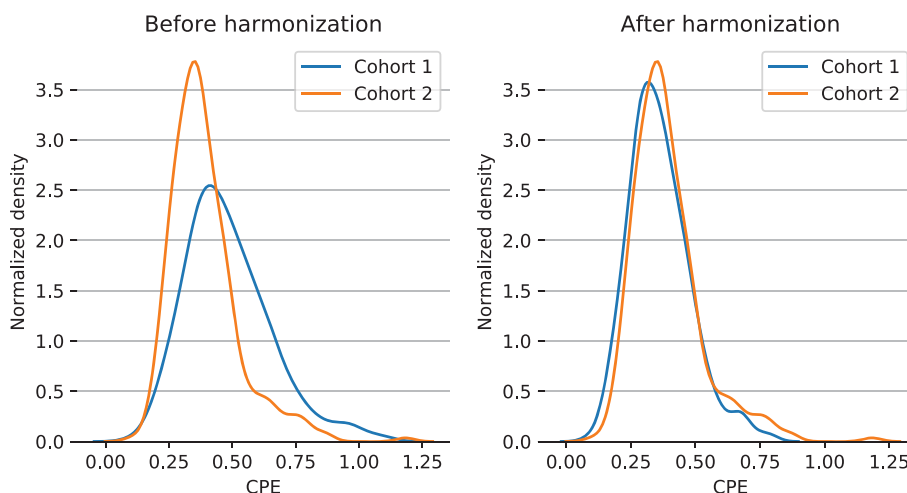


FIGURE 7: The overlap of the kernel density estimations between contralateral parenchymal enhancement in cohort 1 ($n = 394$, blue) and cohort 2 ($n = 302$, orange) significantly increased after harmonization from 57% (left) to 85% (right) ($P < 0.001$).

We provided such harmonization by adjusting the CPE biomarker.^{18,19,32,33} We showed that we were able to adjust this biomarker in our simulation with realistic parameter settings. Compared to the simulation, our phantom study showed slightly more variation after harmonization. This may be because the noise levels in our simulations were based on the SNR measurement from our phantom, which was assessed once at a flip angle of 10° and TR of 4 msec. As a result, the noise varies between acquisition settings in our phantom study, where it does not in our simulation. Another reason may be T₂*-effects, which were not addressed by our simulations. To minimize this potential reason, we chose tubes in our phantom with similar T₂-values and we chose our TE as short as possible on our MR system.

In our clinical data, the improved similarity between CPE values in the cohorts after harmonization was in agreement with the simulations for the parameter settings we were adjusting given the SNR in our images. Therefore, even though the SNR of the MR acquisition is often not optimized for parenchymal tissue, harmonization with real patient cohort data still appears feasible.

The proposed harmonization method is relatively straightforward to implement using the provided description and the article from Haacke et al.²² Although we used seemingly straightforward MR physics, there are several aspects that potentially complicate harmonization of patient data. These aspects include postprocessing on the scanner by vendor software, noise, patient motion, and biological patient

variation. It is promising that, in spite of these potential complications, our results show a good harmonization between patient cohorts.

The duration of the dynamic contrast-enhanced series was comparable in the cohorts. Hence, our study did not investigate the effect of temporal resolution on enhancement features. This is subject to future research. International guidelines prescribe, however, limits to the range of timing in dynamic contrast-enhanced series.^{5,34}

Different contrast agents have different relaxivity properties that might influence enhancement characteristics.³⁵ The contrast agents used in our study (Prohance and Magnevist) have, however, similar relaxivity properties.³⁵

We harmonized the parenchymal enhancement in the contralateral breast. Although we focused on the contralateral breast to exclude cancer-induced enhancement, the same methodology can be applied to the ipsilateral breast.

The effect of harmonization on other enhancement biomarkers, such as radiomics features extracted from the tumor,^{36–38} may also lend themselves to harmonization. In future research, we will investigate the effect of harmonization on these biomarkers.

We chose a model-based harmonization method. The alternative would be a data-driven approach. Such approaches exist; for example, by harmonizing given feature distributions,³⁹ or by harmonizing MR images using deep learning, from which features can then be calculated.⁴⁰ Our model-based approach may have several advantages over data-driven approaches. First, by using a model-based approach, one can anticipate the efficacy of the harmonization under different conditions. Second, data-driven approaches typically require much data. This can be a problem with the prospective use of such methods. For example, in the case of a new MR unit, one needs to gather enough data first in order to perform accurate harmonization.

Limitations

Our study has some limitations. First, we performed our analyses only at 1.5T. Our results may slightly vary at 3T, due to the slightly higher T_1 of parenchymal tissue at 3T and the decreased effect of contrast agent at 3T.^{20,35} However, since the overall behavior of spoiled gradient echo is similar at both field strengths, we expect our results to hold for 3T. Our study shows promising results at B_1^+ field inhomogeneities that are expected at 1.5T.²⁶ These inhomogeneities are higher at higher field strengths.⁴¹ Vendors, however, have acknowledged this and updated their systems accordingly.⁴²

We only gave indirect evidence for the efficacy of the harmonization method in patients. A more direct assessment of the harmonization method in vivo may be a test–retest measurement: scanning the same patient twice or more often with different flip angles and TRs. To fully elucidate the parenchymal enhancement, this would mean scanning the

same patient on different days, since clearance of the contrast agent from the body takes ~ 1 day.^{43,44} Furthermore, even if all these steps would be taken, there are considerable physiological variations in breast parenchyma that occur from day to day,^{45,46} rendering it difficult to control such an experiment.

Conclusion

We showed promising results that harmonization of parenchymal enhancement values can enable accurate comparisons between patients scanned with differences in imaging parameters.

REFERENCES

1. Kuhl CK. The current status of breast MR imaging part I. Choice of technique, image interpretation, diagnostic accuracy, and transfer to clinical practice. *Radiology* 2007;244:356-378.
2. Arasu VA, Miglioretti DL, Sprague BL, et al. Population-based assessment of the association between magnetic resonance imaging background parenchymal enhancement and future primary breast cancer risk. *J Clin Oncol* 2019;37:954-963.
3. King V, Brooks JD, Bernstein JL, Reiner AS, Pike MC, Morris EA. Background parenchymal enhancement at breast MR imaging and breast cancer risk. *Radiology* 2011;260:50-60.
4. Breast Magnetic Resonance Imaging (MRI) Accreditation Program Requirements. <https://www.acraccreditation.org/modalities/breast-mri>
5. Morris EA, Comstock CE, Lee CH. *ACR BI-RADS magnetic resonance imaging*. Reston, VA: American College of Radiology; 2013.
6. El Khoury M, Lalonde L, David J, Labelle M, Mesurolle B, Trop I. Breast imaging reporting and data system (BI-RADS) lexicon for breast MRI: Interobserver variability in the description and assignment of BI-RADS category. *Eur J Radiol* 2015;84:71-76.
7. Grimm LJ, Anderson AL, Baker JA, et al. Interobserver variability between breast imagers using the fifth edition of the BI-RADS MRI lexicon. *Am J Roentgenol* 2015;204:1120-1124.
8. Hylton NM, Gatsonis CA, Rosen MA, et al. Neoadjuvant chemotherapy for breast cancer: Functional tumor volume by MR imaging predicts recurrence-free survival—results from the ACRIN 6657/CALGB 150007 I-SPY 1 TRIAL. *Radiology* 2016;279:44-55.
9. Liao GJ, Henze Bancroft LC, Strigel RM, et al. Background parenchymal enhancement on breast MRI: A comprehensive review. *J Magn Reson Imaging* 2019;51:43-61.
10. Wu S, Weinstein SP, DeLeo MJ, et al. Quantitative assessment of background parenchymal enhancement in breast MRI predicts response to risk-reducing salpingo-oophorectomy: Preliminary evaluation in a cohort of BRCA1/2 mutation carriers. *Breast Cancer Res* 2015;17:1-11.
11. Hu X, Jiang L, Li Q, Gu Y. Quantitative assessment of background parenchymal enhancement in breast magnetic resonance images predicts the risk of breast cancer. *Oncotarget* 2017;8:10620-10627.
12. You C, Peng W, Zhi W, et al. Association between background parenchymal enhancement and pathologic complete remission throughout the neoadjuvant chemotherapy in breast cancer patients. *Transl Oncol* 2017;10:786-792.
13. Luo J, Johnston BS, Kitsch AE, et al. Ductal carcinoma in situ: Quantitative preoperative breast MR imaging features associated with recurrence after treatment. *Radiology* 2017;285:788-797.
14. Knuttel FM, van der Velden BHM, Loo CE, et al. Prediction model for extensive ductal carcinoma in situ around early-stage invasive breast cancer. *Invest Radiol* 2016;51:462-468.
15. Hattangadi J, Park C, Rembert J, et al. Breast stromal enhancement on MRI is associated with response to neoadjuvant chemotherapy. *Am J Roentgenol* 2008;190:1630-1636.

16. Jones EF, Sinha SP, Newitt DC, et al. MRI enhancement in stromal tissue surrounding breast tumors: Association with recurrence free survival following neoadjuvant chemotherapy. *PLoS One* 2013;8:1-8.
17. Vreemann S, Dalmis MU, Bult P, et al. Amount of fibroglandular tissue FGT and background parenchymal enhancement BPE in relation to breast cancer risk and false positives in a breast MRI screening program. *Eur Radiol* 2019;29:4678-4690.
18. van der Velden BHM, Dmitriev I, Loo CE, Pijnappel RM, Gilhuijs KGA. Association between parenchymal enhancement of the contralateral breast in dynamic contrast-enhanced MR imaging and outcome of patients with unilateral invasive breast cancer. *Radiology* 2015;276:675-685.
19. van der Velden BHM, Sutton EJ, Carbonaro LA, Pijnappel RM, Morris EA, Gilhuijs KGA. Contralateral parenchymal enhancement on dynamic contrast-enhanced MRI reproduces as a biomarker of survival in ER-positive/HER2-negative breast cancer patients. *Eur Radiol* 2018;28:4705-4716.
20. Rakow-Penner R, Daniel B, Yu H, Sawyer-Glover A, Glover GH. Relaxation times of breast tissue at 1.5T and 3T measured using IDEAL. *J Magn Reson Imaging* 2006;23:87-91.
21. Giess CS, Yeh ED, Raza S, Birdwell RL. Background parenchymal enhancement at breast MR imaging: Normal patterns, diagnostic challenges, and potential for false-positive and false-negative interpretation. *Radiographics* 2014;34:234-247.
22. Haacke EM, Filletti CL, Gattu R, et al. New algorithm for quantifying vascular changes in dynamic contrast-enhanced MRI independent of absolute T1 values. *Magn Reson Med* 2007;58:463-472.
23. Kim S-Y, Cho N, Park I-A, et al. Dynamic contrast-enhanced breast MRI for evaluating residual tumor size after neoadjuvant chemotherapy. *Radiology* 2018;289:327-334.
24. Hegenscheid K, Schmidt CO, Seipel R, et al. Normal breast parenchyma: Contrast enhancement kinetics at dynamic MR mammography—Influence of anthropometric measures and menopausal status. *Radiology* 2013;266:72-80.
25. Chan S, Su M-YL, Lei F-J, et al. Menstrual cycle-related fluctuations in breast density measured by using three-dimensional MR imaging. *Radiology* 2011;261:744-751.
26. Tsai W-C, Kao K-J, Chang K-M, et al. B₁ field correction of T1 estimation should be considered for breast dynamic contrast-enhanced MR imaging even at 1.5T. *Radiology* 2017;282:55-62.
27. Dietrich O, Raya JG, Reeder SB, Reiser MF, Schoenberg SO. Measurement of signal-to-noise ratios in MR images: Influence of multichannel coils, parallel imaging, and reconstruction filters. *J Magn Reson Imaging* 2007;26:375-385.
28. Yamykh VL. Actual flip-angle imaging in the pulsed steady state: A method for rapid three-dimensional mapping of the transmitted radio-frequency field. *Magn Reson Med* 2007;57:192-200.
29. Otsu N. A threshold selection method from gray-level histograms. *IEEE Trans Syst Man Cybern* 1979;SMC-9:62-66.
30. Gudbjartsson H, Patz S. The Rician distribution of noisy MRI data. *Magn Reson Med* 1995;34:910-914.
31. Pastore M. Overlapping: A R package for estimating overlapping in empirical distributions software • review • repository • archive. *J Open Source Softw* 2018;3:1-4.
32. van der Velden BHM, Elias SG, Bismeyer T, et al. Complementary value of contralateral parenchymal enhancement on DCE-MRI to prognostic models and molecular assays in high-risk ER+/HER2- breast cancer. *Clin Cancer Res* 2017;23:6505-6515.
33. van der Velden BHM, Bismeyer T, Canisius S, et al. Are contralateral parenchymal enhancement on dynamic contrast-enhanced MRI and genomic ER-pathway activity in ER-positive/HER2-negative breast cancer related? *Eur J Radiol* 2019;121:1-6.
34. Mann RM, Kuhl CK, Kinkel K, Boetes C. Breast MRI: Guidelines from the European Society of Breast Imaging. *Eur Radiol* 2008;18:1307-1318.
35. Rohrer M, Bauer H, Mintorovitch J, Requardt M, Weinmann H-J. Comparison of magnetic properties of MRI contrast media solutions at different magnetic field strengths. *Invest Radiol* 2005;40:715-724.
36. Valdora F, Houssami N, Rossi F, Calabrese M, Tagliafico AS. Rapid review: Radiomics and breast cancer. *Breast Cancer Res Treat* 2018;169:217-229.
37. Chitalia RD, Kontos D. Role of texture analysis in breast MRI as a cancer biomarker: A review. *J Magn Reson Imaging* 2019;49:927-938.
38. Chan HM, van der Velden BHM, Loo CE, Gilhuijs KGA. Eigentumors for prediction of treatment failure in patients with early-stage breast cancer using dynamic contrast-enhanced MRI: A feasibility study. *Phys Med Biol* 2017;62:6467-6485.
39. Whitney HM, Li H, Ji Y, Liu P, Giger ML. Harmonization of radiomic features of breast lesions across international DCE-MRI datasets. *J Med Imaging* 2020;7:1.
40. Modanwal G, Vellal A, Buda M, Mazurowski MA. MRI image harmonization using cycle-consistent generative adversarial network. In: Hahn HK, Mazurowski MA, editors. *Medical imaging 2020 Computer diagnosis*, Vol 11314. Bellingham, WA: SPIE; 2020. p 36.
41. Kuhl CK, Kooijman H, Gieseke J, Schild HH. Effect of B₁ inhomogeneity on breast MR imaging at 3.0 T. *Radiology* 2007;244:929-930.
42. Harvey PR, Hoogeveen RM. Multitransmit parallel RF transmission technology setting the benchmark in clinical high-field imaging. http://mri-q.com/uploads/3/4/5/7/34572113/mr_achieva_tx_whitepaper_multitransmit.pdf
43. Bellin M-F, Van Der Molen AJ. Extracellular gadolinium-based contrast media: An overview. *Eur J Radiol* 2008;66:160-167.
44. Aime S, Caravan P. Biodistribution of gadolinium-based contrast agents, including gadolinium deposition. *J Magn Reson Imaging* 2009;30:1259-1267.
45. Aliu SO, Jones EF, Azziz A, et al. Repeatability of quantitative MRI measurements in normal breast tissue. *Transl Oncol* 2014;7:130-137.
46. Arslan G, Çelik L, Çubuk R, Çelik L, Atasoy MM. Background parenchymal enhancement: Is it just an innocent effect of estrogen on the breast? *Diagn Interv Radiol*. 2017;23:414-419.